Block of Single L-type Ca^{2+} Channels in Skeletal Muscle Fibers by Aminoglycoside Antibiotics

CHRISTINE M. HAWS, BRUCE D. WINEGAR, and JEFFRY B. LANSMAN

From the Department of Cellular and Molecular Pharmacology, School of Medicine, University of California, San Francisco, California 94143-0450

ABSTRACT The activity of single L-type Ca^{2+} channels was recorded from cell-attached patches on acutely isolated skeletal muscle fibers from the mouse. The experiments were concerned with the mechanism by which aminoglycoside antibiotics inhibit ion flow through the channel. Aminoglycosides produced discrete fluctuations in the single-channel current when added to the external solution. The blocking kinetics could be described as a simple bimolecular reaction between an aminoglycoside molecule and the open channel. The blocking rate was found to be increased when either the membrane potential was made more negative or the concentration of external permeant ion was reduced. Both of these effects are consistent with a blocking site that is located within the channel pore. Other features of block, however, were incompatible with a simple pore blocking mechanism. Hyperpolarization enhanced the rate of unblocking, even though an aminoglycoside molecule must dissociate from its binding site in the channel toward the external solution against the membrane field. Raising the external permeant ion concentration also enhanced the rate of unblocking. This latter finding suggests that aminglycoside affinity is modified by repulsive interactions that arise when the pore is simultaneously occupied by a permeant ion and an aminoglycoside molecule.

INTRODUCTION

Aminoglycoside antibiotics are a class of large polycationic amino sugars (Berdy et al., 1980). A body of evidence shows that the aminoglycosides inhibit neuromuscular transmission (Timmerman et al., 1959; Dretchen et al., 1972; Wright and Collier, 1977; Singh et al., 1979; Caputy et al., 1981; Enomoto and Maeno, 1981; Fieckers, 1983). While these drugs are thought to inhibit neurotransmission by blocking voltage-gated Ca^{2+} channels, they also block currents through a wide variety of ionic channels, including high-conductance Ca^{2+}-activated K^+ channels (Nomura et al., 1990), mechanotransduction channels in cochlear and vestibular hair cells (Ohmori, 1985; Kroese et al., 1989; Dulon et al., 1989), as well as voltage-gated Ca^{2+} channels (Hino et al., 1982; Suarez-Kurtz and Reuben, 1987; Atchison et al., 1988). Aminoglycoside antibiotics have also been shown to cause certain forms of neurotoxicity through their action on voltage-gated Ca^{2+} channels (Wagner et al., 1987).

The mechanism by which aminoglycosides antibiotics inhibit Ca^{2+} channels, however, is poorly understood. Previous studies have suggested that the polycationic aminoglycosides displace Ca^{2+} from the surface membrane, thereby reducing the availability of permeant ion at the entrance to the channel (Hino et al., 1982; Suarez-Kurtz and Reuben, 1987). This idea is supported by work on phospholipid membranes. Aminoglycosides bind to acidic phospholipids, where they reduce the membrane surface potential (Lüllmann et al., 1980; Brasseur et al., 1984; Chung et al., 1985; Gâbev et al., 1989). In contrast to this purely electrostatic effect, the aminoglycosides may directly block ion fluxes through the conduction pathway. There is, however, little direct evidence for such a mechanism in Ca^{2+} channels.

This study describes the effects of various aminoglycoside antibiotics on the activity of single L-type Ca^{2+} channels recorded from the surface membrane of mouse skeletal muscle fibers. Aminoglycoside antibiotics caused the channel to fluctuate between the open and closed state in a manner suggesting that it blocks the open channel by binding in the pore. We found, however, that blocker affinity depended little on its net charge, but much more strongly on the concentration

Dr. Haws' present address is Cystic Fibrosis Research Laboratory, Stanford University, Stanford, CA 94305.

Dr. Winegar's present address is Department of Anesthesia, School of Medicine, University of California, San Francisco, CA 94143-0648. Address correspondence to Dr J.B. Lansman, Department of Cellular and Molecular Pharmacology, School of Medicine, University of California, San Francisco, CA 94143-0450. E-mail, jeffl@itsa.ucsf.edu.

J. GEN. PHYSIOL. © The Rockefeller University Press • 0022-1295/96/03/421/12 $2.00
Volume 107 March 1996 421–432

of permeant ion in the external solution. The interaction between permeant ion and blocker can be explained by the same ion–ion interactions that contribute to the high rates of ion transport. Some of these results have been reported as an abstract (Winegar et al., 1992).

MATERIALS AND METHODS

Preparation of Single Skeletal Muscle Fibers

Single flexor digitorum brevis (FDB) muscle fibers were dissociated from 17-d old wild type mice (C57BL/6; Simonsen Laboratories, Inc., Gilroy, CA) following the procedure described by Bekoff and Betz (1977). The muscle was dissected free from the plantar surface of the hind limb and suspended for 30 min in DME containing 0.25% collagenase B (Boehringer Mannheim Corp., Indianapolis, IN). The muscle was rinsed with DME supplemented with 5% horse serum and individual fibers were dissociated by drawing the muscle through the fire-polished tip of a Pasteur pipette. Isolated fibers were plated into 35-mm plastic Petri dishes that were coated with Matrigel™ (Collaborative Research, Inc., Waltham, MA) and allowed to adhere to the bottom of the dish.

Electrophysiological Methods

Single-channel activity was recorded from cell-attached patches following the technique described by Hamill et al., (1981). Patch electrodes were pulled from borosilicate capillary tubes (Dynalab Corp., Rochester, NY), the shanks were coated with Sylgard® (Dow Corning, Corning, NY) and the tips heat-polished. Currents were measured with a List EPC-7 amplifier, filtered with an eight-pole Bessel filter (−3 dB at 3 kHz), and recorded onto a 200T PCM data recorder (A.R. Vetter Co., Rebersburg, PA). The current records were analyzed on a laboratory computer (LSI 11/73) after being filtered at 1 kHz and digitized at 5 kHz. All experiments were done at room temperature (~21–23°C).

Solutions

The patch electrode filling solution contained (in millimolar) 150 LiCl, 10 HEPES, 5 EDTA, and 35 glucose. The pH was adjusted to 7.5 by adding tetraethylammonium hydroxide. Li^+ was used as the charge carrier through the channel (Hess et al., 1986), since the sulfate salts of the aminoglycosides were insoluble in the presence of high concentrations of divalent cations. The conductance of the skeletal muscle L-type channel in the presence of 150 mM Li^+ was 12–15 pS, similar to its conductance in the presence of 110 mM Ba^{2+} (Lansman, 1990). This value is considerably smaller than the conductance of the cardiac Ca^{2+} channel, which is ~25 and 45 pS in the presence of 110 mM Ba^{2+} and 150 mM Li^+, respectively (Hess et al., 1986). Moreover, that the conductance is similar in the presence of either Li^+ or Ba^{2+} as the charge carrier, indicates that Li^+ binds with relatively high affinity to the pore.

The bathing solution contained (in millimolar) 150 potassium aspartate, 5 $MgCl_2$, 10 EGTA, 10 HEPES, and 10 glucose. The pH was adjusted to 7.5 with TEA-OH. The isotonic K^+ bathing solution was used to zero the cell's resting potential so that the patch potential was the same as the voltage applied to the electrode. The voltage error introduced by this procedure was generally < 5 mV. An error as large as 10–15 mV was measured in a small number of experiments as a shift in the single-channel *i-V* relation after patch excision. The contribution of this source of error was minimized by rejecting experiments in which there was a change in the single-channel current after excising the patch at the end of an experiment.

Analysis of Channel Block

In recordings from patches on FDB fibers, channel opening probability was low in response to voltage steps that activate inward monovalent currents through the Ca^{2+} channel (~−40 mV). To increase channel open probability, we added the dihydropyridine agonist (+)-S-202-791 (1 μM) to the bathing solution. Shortly after the agonist was added to the bath (< 1 min), channel opening probability during the voltage step increased and individual openings were prolonged (Hess et al., 1984). In many of the experiments, we also applied a strong positive prepulse (~+50 to +70 mV) before stepping the patch potential to the test potential (Lansman, 1990). The positive prepulse increased channel activity during the subsequent voltage step and made it possible to record channel activity over a wider range of voltages than is possible using a single step protocol.

The blocking actions of the aminoglycosides were studied by adding the drug to the patch electrode filling solution. Channel openings were sufficiently prolonged in the presence of the dihydropyridine agonist so that block could be resolved as discrete transitions between the open and closed states. We performed control experiments to test whether the presence of the agonist influenced the blocking kinetics. The durations of open and blocked times were measured in the presence of either low or high concentrations of the agonist (0.5 or 10 μM). The measured blocking kinetics were within 2% and, consequently, not affected by the 20-fold difference in the bath agonist concentration (data not shown). In an additional set of controls, we found that the blocking kinetics were also unaffected by including 10 mM each of EDTA and EGTA in the patch electrode filling solution. This ruled out the possibility that a metal ion contaminant contributed to the channel block observed in the presence of aminoglycoside.

To analyze the kinetics of the current fluctuations, transitions between the open and closed states were detected as crossings of a threshold level set half way between the open and closed channel levels (Colquhoun and Sigworth, 1983). Records were not used for analysis if they contained multiple, superimposed bursts of openings. Channel openings within a burst were generally well-resolved within the 1 kHz bandwidth of the recording system. Because of the presence of brief closings in the single-channel records, however, we corrected the open times for missed closings when >20% of the events were missed. A correction for missed brief closings was necessary because they would cause the mean open time to be overestimated. The correction used was similar to the one described by Colquhoun and Sigworth (1983) and Blatz and Magleby (1986). The ratio of the number of missed closings to the total number of closings was calculated as

$$1 - \exp(-D/\mu_c) \quad (1)$$

where D is the dead time of the recording system (~200 μs) and μ_c is the mean substate duration obtained from the fit to the his-

togram of closed times. Mean open times were corrected by multiplying the uncorrected mean open time by the ratio given by (Eq. 1) and then subtracting the duration of all missed closings.

The correction for missed blockages was tested in simulations (Winegar et al., 1991). Single-channel data were simulated using the rate constants obtained from analysis of the blocking kinetics. The rates were used to specify a two-state random process and Gaussian noise was added to the simulated records. The records were filtered at one-fifth the sampling rate and analyzed with the half-threshold detection method. After correction for missed events, the measured rates were within 10% of the rates that were originally used to generate the simulated records.

RESULTS

The chemical structures of the aminoglycosides used in this study are shown in Fig. 1. Aminoglycoside antibiotics consist of two or more amino sugars joined to a hexose nucleus by a glycosidic linkage. The different families of aminoglycosides differ in the number of amino sugars. As shown in Fig. 1, neomycin has three amino sugars, while kanamycin and gentamicin have two each. Streptomycin and dihydrostreptomycin differ from the other aminoglycosides in that the hexose group is not centrally located and it is streptidine, rather than a 2-deoxystreptamine. The aminoglycosides also differ in their net charge at physiological pH, which ranges from +4.4 for neomycin to +2 for streptomycin and dihydrostreptomycin (Table I). In the experiments described below, we investigated the blocking actions of each of the aminoglycosides shown in Fig. 1 to obtain information on the effect of aminoglycoside structure on the blocking mechanism.

Fig. 2 shows the effects of externally applied aminoglycosides on the single-channel currents carried by Li^+. Single-channel activity was recorded during a voltage step from a holding potential of −80 mV to a test potential of −50 mV. The bathing solution contained the dihydropyridine agonist +(S)-202-791 to prolong the channel open time. In control recordings made with no aminoglycoside in the electrode solution (*top record*), channel activity appeared as well-resolved openings with an amplitude of ~−1.5 pA at −50 mV. In recordings made with an electrode filling solution containing 1 mM of an aminoglycoside, however, there were many brief closures in the single-channel currents (records 2–6). Fig. 2 shows that 1 mM of either neomycin or kanamycin produced many more brief closures than did an equal concentration of either streptomycin, dihydrostreptomycin, or gentamicin. These brief closures represent individual blocking events that arise from the repetitive blocking and unblocking of the channel by a single aminoglycoside molecule. The experiments described below tested the validity of the channel blocking model.

Concentration Dependence of Block

As a starting point in the analysis, we adopted a simple model for open-channel block that has proved useful for studying the mechanism of drug block in a variety

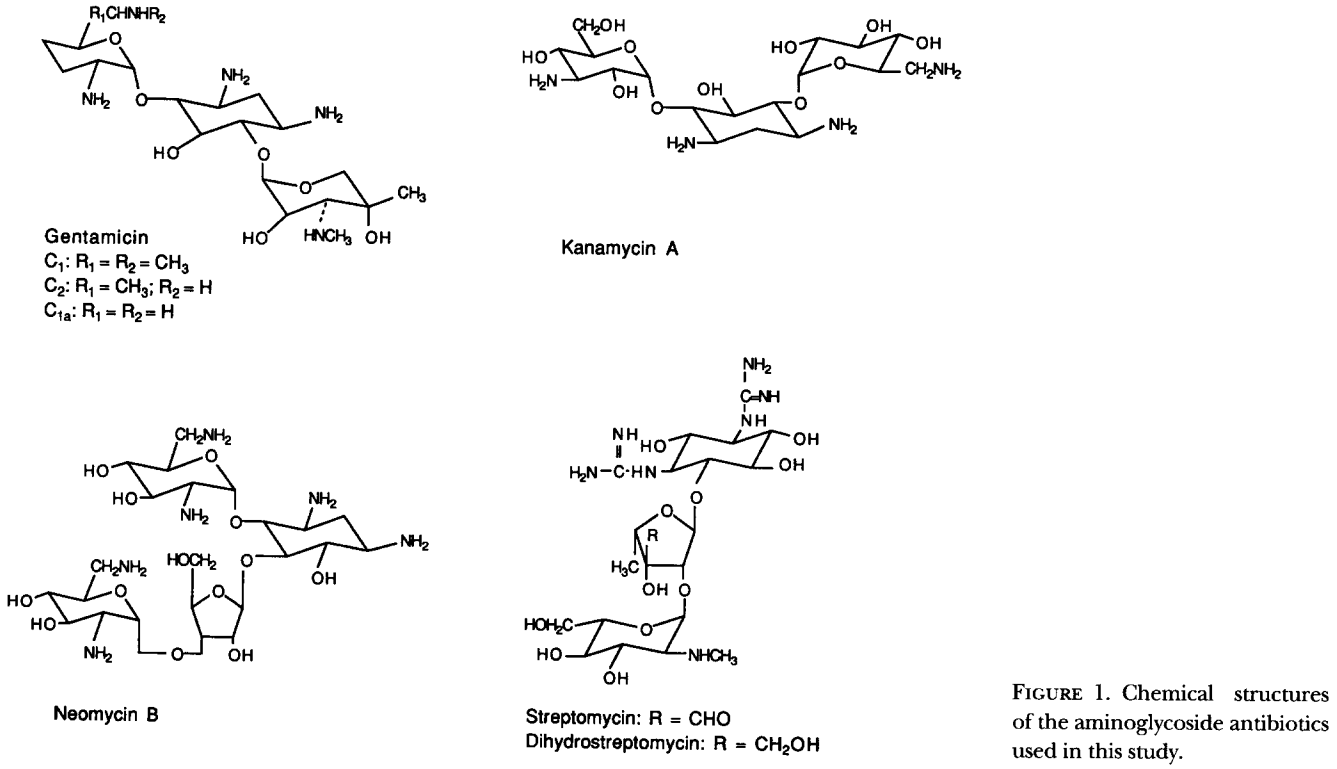

FIGURE 1. Chemical structures of the aminoglycoside antibiotics used in this study.

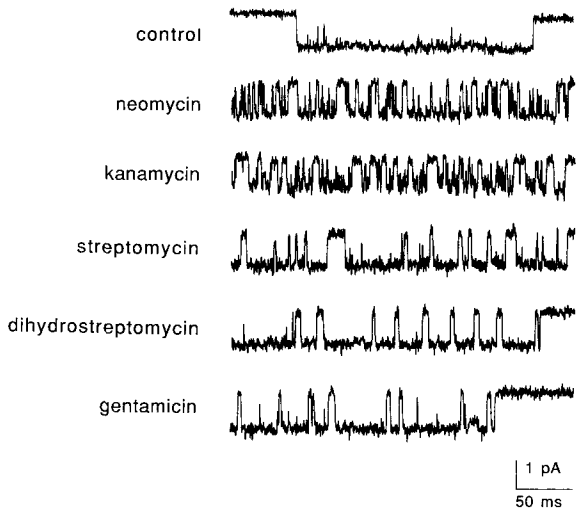

FIGURE 2. The blocking actions of various aminoglycoside antibiotics on single L-type Ca^{2+} channels. Channel activity was recorded in response to a voltage step to −50 mV from a holding potential of −80 mV. The patch electrode contained 150 mM LiCl to which was added 1 mM of the indicated aminoglycoside. The bathing solution contained isotonic K-aspartate and the dihydropyridine agonist, (+)-S-202-791. Each record is from a different cell-attached patch. Currents were filtered at 1 kHz and sampled at 5 kHz.

of ion channels (Armstrong, 1969; Neher and Steinbach, 1978):

$$O \underset{k_{-b}}{\overset{k_b}{\leftrightarrow}} OB, \qquad (2)$$

where O is the open state, OB is the blocked state of the channel, and k_b and k_{-b} are the rates of blocking and unblocking, respectively. We neglected closed states in the activation pathway, since there were relatively few closures in the single-channel records in the absence of blocker. The relatively low rate of channel closing in control recordings ensured that the large majority of closures in the presence of aminoglycoside reflected true blockages. The low rate of closing also made it unlikely that a closed blocked state contributed substantially to the observed kinetics.

The simple blocking model makes several predictions about the kinetics of block. First, histograms of open and closed times are exponentially distributed, reflecting the existence of a single open and a single blocked state. Second, the inverse of the mean open time is linearly related to the concentration of blocker and is a measure of the bimolecular blocking rate coefficient. Third, the inverse of the mean closed time is independent of drug concentration. These predictions were tested below by examining the effects of aminoglycoside concentration on channel open and closed times.

Fig. 3 shows the effects of varying the aminoglycoside concentration on the the single-channel currents carried by Li^+. Each record is from a different experiment with the indicated concentration of aminoglycoside added to the patch electrode. As expected for a reaction between an aminoglycoside and the open channel, increasing the concentration of aminoglycoside increased the number of blockages in the single-channel records. Fig. 4 shows the analysis of the blocking kinetics in the presence of different concentrations of kanamycin. We chose to analyze the block produced by kanamycin because the blocking events were well-resolved. Fig. 4 *A* shows that the open (*left*) and closed time (*right*) histograms were well fit by single exponentials, consistent with the existence of a single open and a single blocked state. The smooth curves drawn through

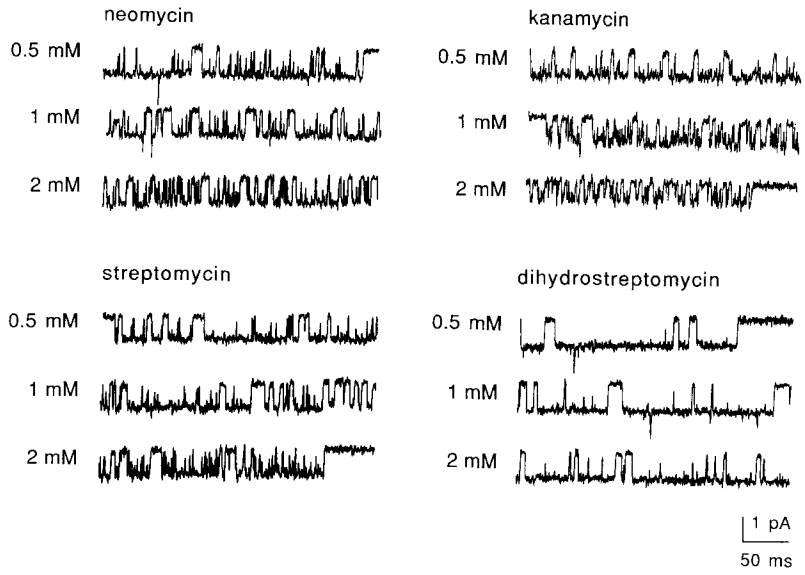

FIGURE 3. Effect of aminoglycoside concentration on the single-channel currents. Each record is from a different patch with the indicated concentration of antibiotic. The patch electrode contained 150 mM LiCl. The bathing solution contained isotonic K-aspartate and the dihydropyridine agonist, (+)-S-202-791. Each record is from a different cell-attached patch. Current records were filtered at 1 kHz and sampled at 5 kHz.

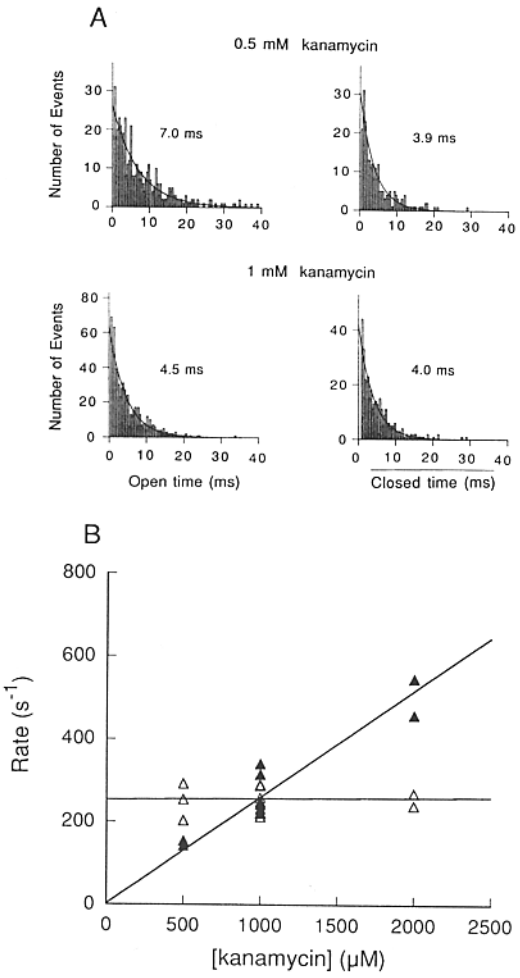

FIGURE 4. Dependence of the blocking kinetics on the concentration of kanamycin. (*A*) Histograms of open and blocked times measured at −40 mV from two experiments in which the patch electrode contained either 0.5 mM (*top*) or 1 mM (*bottom*) kanamycin. The smooth curves through each histogram represent the maximum likelihood fit to a single exponential with the indicated time constant. (*B*) The inverse of the mean open times (*filled triangles*) and closed times (*open triangles*) obtained from the maximum likelihood fits to the lifetime histograms plotted as a function of the concentration of kanamycin in the patch electrode. The straight line through the blocking rate data is the least squares fit with a slope of $\sim 2.6 \times 10^5$ $M^{-1}s^{-1}$. The fit was constrained to pass through the origin. The horizontal line through the unblocking rate data (*open triangles*) corresponds to a rate of ~ 254 s^{-1}.

the histograms show the maximum likelihood fit to a single exponential with the indicated time constants. Fig. 4 *A* also shows that increasing the concentration of kanamycin from 0.5 to 1 mM reduced the time constant obtained from the fit of the open time histogram, but had little effect on the closed time constants. Fig. 4 *B* shows the results that were obtained from a number of recordings with different concentrations of kanamycin in the patch electrode. The inverses of the mean open (τ_o^{-1}, *filled triangles*) and closed times (τ_c^{-1}, *open triangles*) were plotted as a function of the kanamycin concentration. The apparent blocking rate (τ_o^{-1}) increased linearly with the kanamycin concentration, as expected for a reaction with bimolecular kinetics. The slope of the least squares regression line gave a second-order blocking rate coefficient $k_b = \sim 2.6 \times 10^5$ M^{-1} s^{-1}. The fit was constrained to pass through the origin because there were very few intrinsic channel closings that would have been included in the analysis of individual bursts. As expected for a first order process, the unblocking rate (τ_c^{-1}) did not depend on the concentration of kanamycin. The inverse of the mean closed times were averaged and gave an apparent first-order unblocking rate for kanamycin at −40 mV of $k_{-b} = \sim 254$ s^{-1}. The equilibrium dissociation constant was obtained as the ratio k_{-b}/k_b and was $K_D = \sim 1.0$ mM for kanamycin at −40 mV.

Table I shows the equilibrium and kinetic constants obtained from the analysis of the block produced by kanamycin and the other aminoglycoside antibiotics. The data in Table I show that the various aminoglycosides differed in the magnitude of the blocking rate coefficients. Kanamycin and neomycin had the largest blocking rate coefficients, which are roughly an order of magnitude greater than gentamicin or streptomycin. The blocking rate coefficients followed the sequence, neomycin > kanamycin > streptomycin >> dihydrostreptomycin ~ gentamicin. This sequence corresponds roughly to an increase in the blocking rate with an increase in the number of amino sugars on the aminoglycoside molecule. The data in Table I also show that the unblocking rates were virtually the same for all of the aminoglycosides (~ 270 s^{-1}), except for gentamicin which had a considerably higher unblocking rate (~ 430 s^{-1}). The lack of a dependence of the unblocking rate on the particular aminoglycoside is noteworthy, since these drugs differ in their net charge at physiological pH (see below). Apparently, differences in equilibrium affinity arise primarily from differences in the rate of blocker association with the channel and not from the stability of the aminoglycoside-channel complex.

Voltage Dependence of the Aminoglycoside Block

The aminoglycosides have a net charge at physiological pH which ranges from +4.4 (neomycin) to ~+2.0 (streptomycin and dihydrostreptomycin). According to the channel blocking model proposed by Woodhull (1974), the effects of membrane potential can be explained in terms of its contribution to the free energy of blocker binding to its site in the channel. As pointed out above, aminoglycosides with a high net charge dissociate from their binding site just as rapidly as those with less net charge. This lack of an effect of net charge

TABLE I

Aminoglycoside Blocking Parameters

Antibiotic	Net charge	k_{on} (M^{-1} s^{-1})		e-fold Δ	k_{off} (s^{-1})	e-fold Δ	K_d	
	*pH 7.4**	*−40 mV*	r^2	*mV*	*.2–2 mM*	*mV*	*mM*	*n*
Neomycin	+4.4	3.4×10^5	.94	42	267 ± 19	50	0.8	5
Kanamycin	+2.4	2.5×10^5	.85	31	289 ± 11	42	1.0	8
Streptomycin	+2	1.2×10^5	.93	70	249 ± 36	38	2.1	4
Dihydrostreptomycin	+2	2.8×10^4	.86	—	281 ± 15	57	10.1	7
Gentamicin	+3.5	3.8×10^4	.81	—	428 ± 77	54	11.1	4

Data from aminoglycoside block of L-type Ca^{2+} channels at a test potential of −40 mV. Values of k_{off} represents the mean ± SE. Dashed lines in the voltage dependence data columns signify kinetic measurements that were not affected by voltage.

*From Josepovitz et al. (1982) and Kroese et al. (1989). Kanamycin net charge is presumed to be similar to amikacin (+2.39 at pH 7.4). Amikacin is a derivative of kanamycin A. Dihydrostreptomysin is presumed to have a net charge close to streptomycin.

on blocking would be consistent with the model, however, if drug dissociation from the channel occurred over an insignificant fraction of the total field. Alternatively, only one charged group that is common to all of the aminoglycosides participates in the blocking reaction. To distinguish between these possibilities, the blocking kinetics were measured at different membrane potentials to obtain information on the voltage sensitivity of the individual steps of blocking reaction.

Fig. 5 shows the single-channel activity that was recorded in four experiments in the presence of either neomycin, kanamycin, streptomycin, or dihydrostreptomycin. As shown in Fig. 5, the test potential was varied over the voltage range −20 to −70 mV in each re-

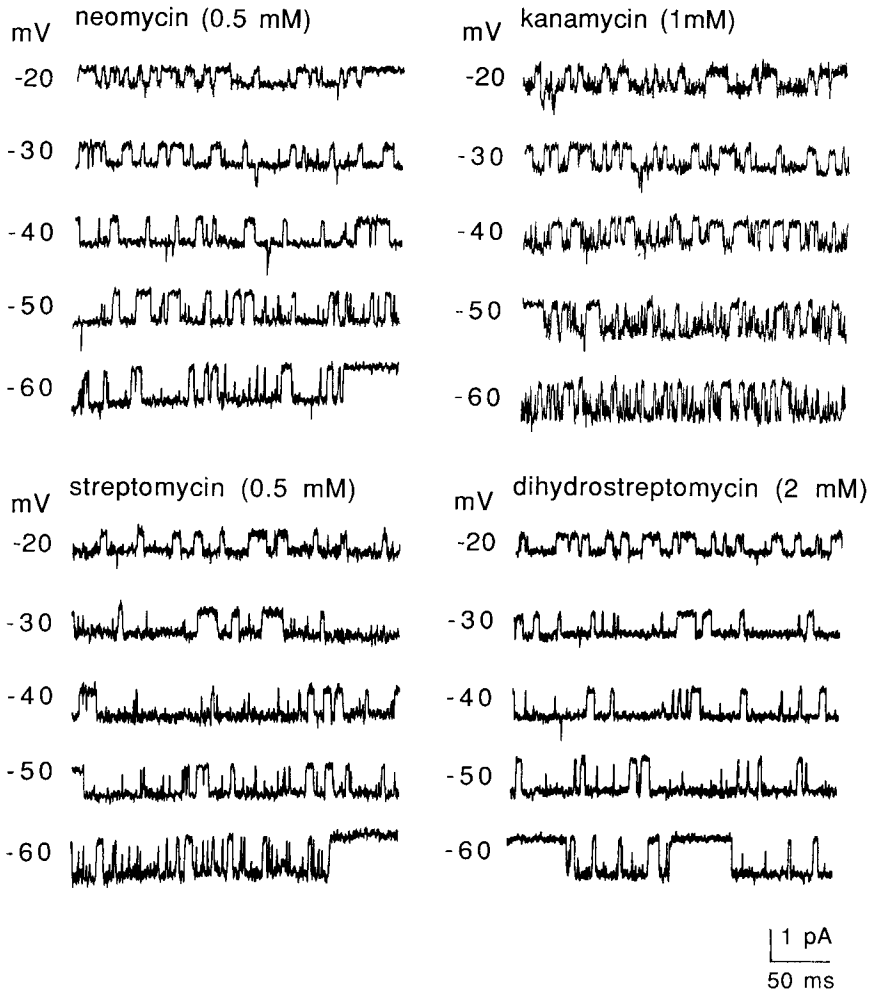

FIGURE 5. Voltage-dependence of the blocking kinetics in the presence of either neomycin, kanamycin, streptomycin, or dihydrostreptomycin. Each of the four panels shows a single experiment with the indicated concentration of antibiotic. The patch electrode contained 150 mM LiCl. The bathing solution contained isotonic K-aspartate and (+)-S-202-791. Currents were recorded in response to voltage steps to the indicated potential from a holding potential of −80 mV. Current records were filtered at 1 kHz and sampled at 5 kHz.

cording. As can be seen in the records, the number of closures increased as the test potential was made progressively more negative. Open and closed times were measured from the records and used to construct histograms which were then fit with a single exponential. Fig. 6 shows the inverses of the mean open and closed times obtained from the exponential fits plotted as a function of the test pulse potential (different symbols are for different aminoglycosides). Fig. 6 *A* shows that, although the aminoglycosides differed in the absolute value of their blocking rate, the blocking rate increased with hyperpolarization. An increase in the blocking rate with hyperpolarization can be explained by an enhanced rate of entry of the positively charged blocking particle to its binding site under the influence of the applied membrane field (Woodhull, 1974). Fig. 6 *B* shows, however, that the unblocking rate also increased with hyperpolarization. If an aminoglycoside binds to a site located in the membrane field, hyperpolarization would be expected to lower the blocking rate. This latter finding is not easily reconciled with the basic Woodhull model, since it would require that the negative membrane potential effectively repelled the positively charged blocker. Fig. 6 *B* also shows that the voltage dependence of unblocking was the same for all of the aminoglycosides (~*e*-fold change per 50 mV).

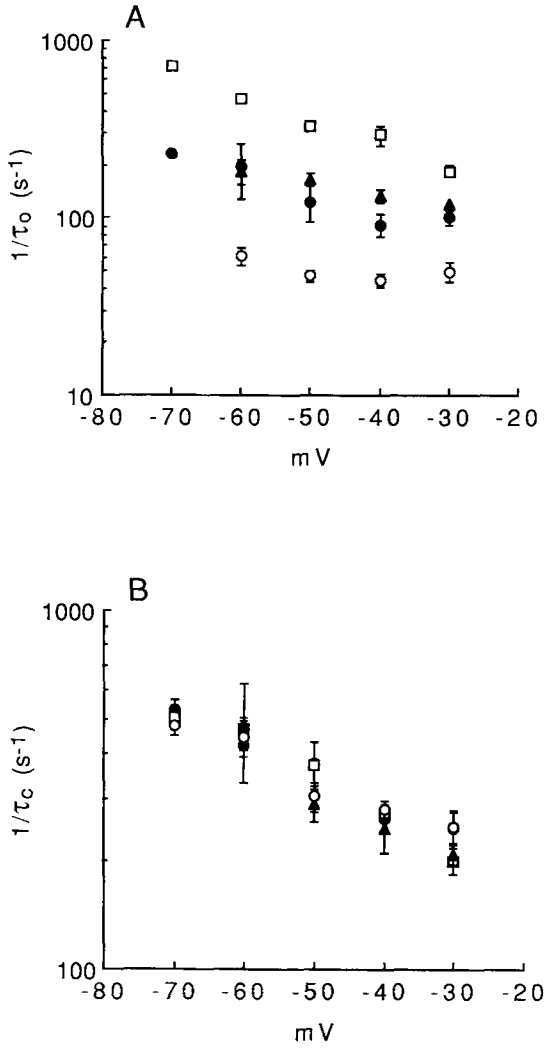

FIGURE 6. Effect of membrane potential on the blocking kinetics. (*A*) Voltage-dependence of the blocking rates ($1/\tau_o$). (*B*) Voltage dependence of the unblocking rates ($1/\tau_c$). The slopes of the relations are given in Table I.

An increase in the rate of unblocking with hyperpolarization has previously been interpreted as the ability of a charged blocker to exit into the interior of the cell (e.g., Lansman et al., 1986). This interpretation seems unlikely here because the cross-sectional area of the aminoglycoside molecule (~52–88 Å^2, Brasseur et al., 1984) is much larger than the pore of the skeletal muscle Ca^{2+} channel, which is estimated to be ~6 Å^2 at its narrowest point (McCleskey and Almers, 1985). Unless binding of an aminoglycoside causes a large increase in pore size, it is not likely to pass through the channel at a finite rate. Consequently, an aminoglycoside is likely to leave its blocking site by returning back to the external solution.

Effect of Permeant Ion Concentration

The results presented so far suggest that the aminoglycoside binding site is in the channel, but they provide no information on whether the site is in the ion permeation pathway. If the binding site is located in the permeation pathway, then the probability that an aminoglycoside can enter and bind to the site will depend on whether the site is occupied by a permeant ion. In these experiments, we measured the open and blocked times in the presence of a fixed concentration of kanamycin (1 mM), but varied the concentration of Li^+ in the electrode. Li^+ was replaced with the impermeant cation, tetraethylammonium ion (TEA^+), so as to maintain a constant ionic strength. In some experiments, however, sucrose was used to replace Li^+ rather than TEA.

Fig. 7 shows that the blocking rate (*filled symbols*) was reduced as the concentration of Li^+ in the electrode was increased. The smooth line is the best fit for Li^+ binding to a single site in the channel (details in legend, Fig. 7). The fit gave a $K_{D(Li)}$ = 110 mM and a maximum blocking rate of 639 s^{-1} in 0 mM Li^+. The probability that the binding site is vacant can be estimated independently from the single-channel conductance, which reflects the probability that the channel is occupied by a second permeant ion (Almers and McCleskey, 1984; Hess and Tsien, 1984; Lansman et al., 1986; Kou and Hess, 1993*b*). A fit of the plot of the single-channel conductance vs the Li^+ concentration gave val-

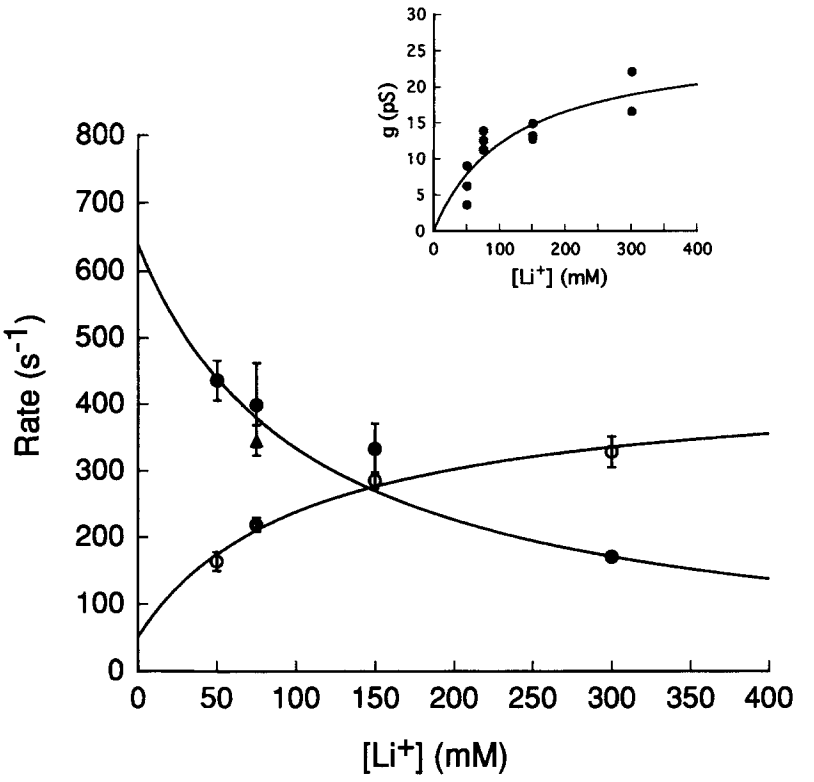

FIGURE 7. Effect of the concentration of external Li^+ on the blocking kinetics. The patch electrode contained 1 mM kanamycin. The blocking rates (*filled symbols*) and unblocking rates (*open symbols*) are plotted as a function of the concentration of Li^+ in the electrode. The data were obtained at a test potential of −40 mV. LiCl was replaced by TEA-Cl (*circles*) to maintain constant ionic strength or sucrose (*triangles*) to vary the ionic strength. The curve through the blocking rate ($1/\tau_o$) data is drawn according to

$$1/\tau_o = k_1/\{(1 + [Li^+]/K_{D(Li)})\}$$

where k_1 is the maximum blocking rate in the absence of permeant ion and $K_{D(Li)}$ is the apparent Li^+ affinity. The best fit was obtained with k_1 = 639 s^{-1} and a $K_{D(Li)}$ = 110 mM Li^+. The curve through the unblocking ($1/\tau_c$) rate data is drawn according to

$$1/\tau_c = k_1 + \{(k_2 - k_1) \times ([Li^+]/(K_{D(Li)^*} + [Li^+]))\},$$

where k_1 is the unblocking rate in low Li^+ concentration, k_2 is the maximum unblocking rate, and $K_{D(Li)^*}$ is the apparent Li^+ affinity. The best fit was obtained with k_1 = 51 s^{-1}, k_2 = 437 s^{-1} and $K_{D(Li)^*}$ = 106 mM. (*Inset*) The single-channel conductance as a function of the external concentration of Li^+. The solid curve was drawn according to

$$g = g_{max} \times \{[Li^+]/(K_{D(Li)} + [Li^+])\}$$

where g_{max} is the maximum conductance and $K_{D(Li)}$ is the affinity for Li^+. The best fit was obtained with g_{max} = 26 pS and K_D = 119 mM.

ues of g_{max} = 26 pS and $K_{D(Li)}$ = 119 mM (details in legend, Fig. 7). Thus, the Li^+ affinity estimated from the reduction in the blocking rate is very similar to that obtained from the saturation of the single-channel conductance. This is consistent with the idea that the aminoglycoside blocker occupies a site that may also be occupied by Li^+ during ion transport.

In a previous study of the block of cardiac Ca^{2+} channels by metal cations, raising the permeant ion concentration was found to enhance the rate of blocker exit from the pore (Lansman et al., 1986). The ability of permeant ion to enhance dissociation of blocker was suggested to involve ion-ion interactions at the high affinity Ca^{2+} binding site (Lansman et al., 1986; Kou and Hess, 1993*a*,*b*). Fig. 7 shows that the aminoglycoside unblocking rates (open symbols) increased as the Li^+ concentration was raised. The unblocking rates were fit assuming one-to-one binding with an apparent $K_{D(Li)^*}$ = 106 mM. The enhancement of the rate of unblocking by external Li^+ indicates that the effect of Li^+ is more complicated than competition for a single site. This effect is consistent, however, with a model in which occupancy of a site by Li^+ destabilizes the binding of the aminoglycoside molecule. While it is possible that Li^+ binds to a site that is remote from the aminoglycoside binding site, the site is not likely to be located more externally than the aminoglycoside binding site. If this were the case, raising Li^+ would slow the rate of unblocking by trapping the aminoglycoside molecule in the channel. Regardless of its precise mechanism, however, the rate of unblocking is expected to be quite low in the absence of permeant ion (~50 s^{-1}).

Effect of External pH

The aminoglycosides are known to adsorb to the surface membrane where they bind to negatively charged groups and reduce the negative surface potential (Chung et al., 1985; Gâbev et al., 1989). Although we have assumed that an aminoglycoside molecule binds in the channel, it may also bind outside the channel to negatively charged lipids. We performed experiments in which the external pH (pH_o) was varied to alter the net charge on the aminoglycoside molecule. Since the ability of the aminoglycosides to bind to negatively

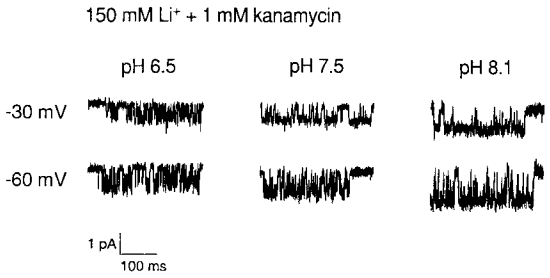

FIGURE 8. The effects of external pH on the block produced by 1 mM kanamycin. The patch electrode contained 150 mM LiCl at the indicated pH_o. The bathing solution contained isotonic K-aspartate and (+)-S-202-791. Currents were recorded in response to voltage steps to either −30 or −60 mV from a holding potential of −80 mV. Currents were filtered at 2 kHz and sampled at 10 kHz.

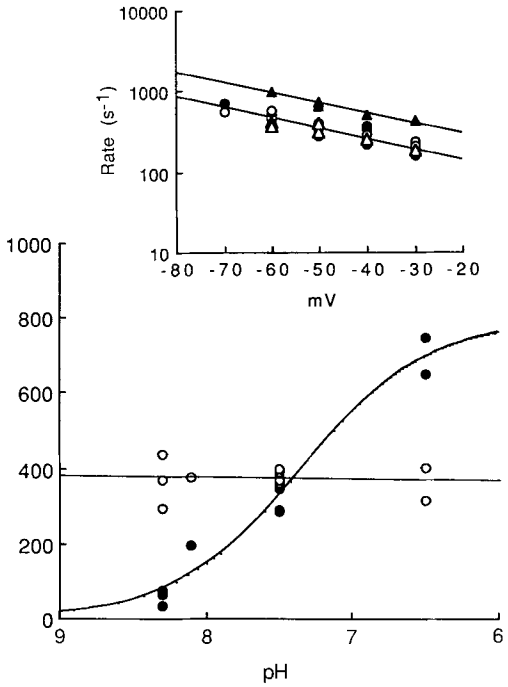

FIGURE 9. Dependence of the kanamycin blocking kinetics on external pH. The blocking rate ($1/\tau_o$) (*filled circles*) and unblocking rate ($1/\tau_c$) (*open circles*) plotted as a function of the external pH. The patch electrode contained 150 mM Li^+ and 1 mM kanamycin. Open and closed closed times were measured at a test potential of −50 mV. The dependence of the apparent blocking rate ($1/\tau_o$) on pH_o was fit to a relation describing the titration of a single site with a pK_a of ~pH 7.35 and a maximum blocking rate of ~800 s^{-1}. The horizontal line was drawn by eye through the unblocking rate data. (*Inset*) Dependence of blocking rates at pH 7.5 (*filled circles*) and pH 6.5 (*filled triangles*) and the unblocking rates at pH 7.5 (*open circles*) and pH 6.5 (*open triangles*) on membrane potential. The patch electrode contained 1 mM kanamycin. The blocking rates at pH 6.5 and 7.5 increased ~*e*-fold per 33 and 35 mV, respectively.

charged lipids depends strongly on their net charge, their binding affinity would be greatly reduced at alkaline pH.

Fig. 8 shows the effects of pH_o on the block produced by 1 mM kanamycin. When the pH_o was increased from 6.5 to 8.1, the number of blockages produced by kanamycin decreased. Note, however, that the duration of the individual blockages did not markedly change. Raising pH_o from 6.5 to 8.1 also increased the amplitude of the single-channel current (Pietrobon et al., 1989). Fig. 9 shows the results of the analysis of the effects of pH_o on the kanamycin blocking kinetics. We found that lowering pH_o greatly enhanced the blocking rate (*filled symbols*). The blocking rate data were fit with a curve that describes the titration of a single site with a pK_a = ~7.3. If pH_o altered the concentration of an active drug species with a pK_a = 7.3, then changes such as those observed in the blocking rate would be expected simply on the basis of the change in blocker concentration. Fig. 9 also shows that changing pH_o over the range 6.5 to 8.1 had little effect on the unblocking rate (*open symbols*). The absence of an effect of pH_o on unblocking is consistent with the finding that aminoglycoside affinity does not depend on its net charge. Fig. 9 (*inset*) shows that the steepness of the relation between the rate of unblocking and membrane potential was the same at pH 6.5 and 7.5. This provides further evidence that the net charge of an aminoglycoside does not determine the voltage dependence of block by a simple contribution to the free energy of binding.

DISCUSSION

The results presented in this paper show that the aminoglycosides inhibit L-type Ca^{2+} channels by producing discrete channel closures. We found no evidence to support a mechanism in which aminoglycosides reduced the permeant ion concentration near the entrance to the channel by screening fixed negative charges, as proposed by Suarez-Kurtz and Rueben (1987). Although the concentrations of aminoglycosides used in this study would have substantially reduced the electrostatic surface potential (Chung et al., 1985), there was no change in the amplitude of the single-channel current over the concentration range studied. Because the effectiveness in screening surface charge is an exponential function of blocker charge, the blocking potencies of aminoglycosides would also be expected to vary according to their net charge. The results showed, however, that the block produced by neomycin, with a net charge of +4.4, was as strong as that produced by kanamycin, which has a net charge of +2.4 at the same pH. These observations, together with

the observation of discrete blocking events in the presence of aminoglycosides, are not easily explained by a charge screening mechanism.

Mechanism of Block

The blocking kinetics were well described by a simple model of open-channel block. Single exponentials fit the histograms of open and blocked times, indicating that there is a single open and a single blocked state. The inverse of the mean open time varied linearly with aminoglycoside concentration and gave a second-order blocking rate coefficient of $k_b = \sim 2.6 \times 10^5\ M^{-1}s^{-1}$. In addition, the inverse of the mean blocked times were concentration-independent and gave an unblocking rate which ranged from 250–290 s^{-1} at −40 mV for all of the aminoglycosides studied, except gentamicin, which had a somewhat higher rate. The results also showed that the blocking rate increased with hyperpolarization in a manner consistent with the movement of a positively charged blocker from the external solution to a binding site located within the membrane field. That the binding site is located within the ion conduction pathway was suggested by the observation that increasing the permeant ion concentration reduced the rate of entry of an aminoglycoside into the pore.

The observation that all of the aminoglycosides had more or less identical unblocking rates suggests that only a portion of an aminoglycoside binds within the pore. A similar interpretation was reached by Nomura et al. (1990) who compared the blocking actions of aminoglycosides and simple alkylamines on Ca^{2+}-activated K^+ channels incorporated into planar bilayers. They showed that the electrical distances obtained from the voltage dependence of block were the same for aminoglycosides and alkyldiamines, but the distances were twice the size of those estimated from the block produced by alkylmonoamines. Nomura et al. (1990) concluded that the two amino groups of the central 2-deoxystreptamine of neomycin and kanamycin entered into the channel to block ion conduction. Our results showed, however, that streptomycin and dihydrostreptomycin, which have a streptadine rather than a 2-deoxystreptamine, bound as tightly as neomycin or kanamycin. Thus, the central hexose group cannot by itself determine aminoglycoside residence time in the Ca^{2+} channel pore. An alternative explanation is that only one of the amino groups entered into the pore to block the channel. The participation of only one amino group in the blocking reaction is supported by the finding that the apparent pK_a of the blocking particle is close to the pK_a of the free amino groups at positions 2 and 3 of kanamycin ($pK_a = \sim 7.5$; Dorman et al., 1976). If only one of the free amino groups acts as the blocking particle, then the observed increase in the blocking rate with the number of amino groups would simply reflect the increase in the number of possible ways for an aminoglycoside to interact with the channel.

The pore blocking model that has been proposed does not easily account for the enhanced rate of aminoglycoside exit back to the external solution at negative potentials. One possibility is that blocker affinity depends on the occupancy of the pore by permeant ion. It is well-established that Ca^{2+} channel selectivity involves the binding of divalent cations to a high affinity site located in the pore (reviewed by Tsien et al., 1987). To account for the high rates of ion transport, models of ion permeation in Ca^{2+} channels have postulated the existence of multiple sites located within the pore and an enhanced rate of dissociation when the pore is multiply occupied (Almers and McCleskey, 1984; Hess and Tsien, 1984; but see Armstrong and Neyton, 1992). Evidence for such ion-ion interactions has come from studies of Ca^{2+} channel block by metal cations where occupancy of the pore by permeant ion was found to speed blocker exit from the pore (Lansman et al., 1986; Kou and Hess, 1993*a,b*). Kou and Hess (1993*b*) characterized these ion–ion interactions in terms of an "enhancement site" that is located at the high affinity binding site(s). The present results are consistent with Li^+ acting at the enhancement site to reduce the affinity of an aminoglycoside bound to the high affinity site. The enhancement effect, however, differs from that observed when small transition metals, such as Cd^{2+} and Mg^{2+}, block the pore. These metal ions are able to dissociate from the pore by passing through the channel to the inside of the cell (Lansman et al., 1986; Kou and Hess, 1993*a,b*). By contrast, occupancy of the pore by permeant ion apparently enhances the dissociation of an aminoglycoside back to the external solution. In this regard, the pore appears to deviate from strict single-file behavior. That there was no evidence for "lock-in" of an aminoglycoside when the external permeant ion concentration was raised, also suggests that there is no restriction on the forward movement of permeant ion when the blocking site is occupied. These deviations from single-file behavior suggest a permeation model in which both permeant ion and blocker complex with a single binding site (Armstrong and Neyton, 1992).

Recent studies of cloned Ca^{2+} channels have localized the high affinity binding site to four glutamate residues in the pore-forming region of the α subunit (Kim et al., 1993; Yang et al., 1993). Evidence suggests that the high affinity binding site is located close to the external surface (Kou and Hess, 1993*b*). The results of this study suggest a model in which one of the positive charges of an aminoglycoside enters into the pore and complexes with the four glutamates making up the binding site. We suggest that a three position amino

group complexes with the high affinity site, leaving two amino sugars protruding out of the pore. Unblocking may require only that the amino group rotates out of the pore, a step which would involve a negligible fraction of the field. The putative kanamycin binding site of the enzyme, kanamycin nucleotidyltransferase, is made up of a ring of seven negatively charged glutamates and aspartates, which also contribute to the Zn^{2+} binding site (Sakon et al., 1993). The blocking actions of aminoglycosides may, therefore, reflect their ability to interact with specific divalent cation binding sites, rather than diffuse negative charges.

This work was supported by the Muscular Dystrophy Foundation and the Office of Army Research (JBL). C.M. Haws was supported by a California Heart Association Fellowship.

Original version received 16 March 1995 and accepted version received 8 December 1995.

REFERENCES

Almers, W., and E.W. McCleskey. 1984. Non-selective conductance in calcium channels of frog muscle: calcium selectivity in a single-file pore. *J. Physiol. (Lond.).* 353:585–608.

Armstrong, C.M. 1969. Inactivation of the potassium conductance and related phenomenon caused by quaternary ammonium ion injected in squid axons. *J. Gen. Physiol.* 54:553–575.

Armstrong, C.M., and J. Neyton. 1992. Ion permeation through calcium channels: a one-site model. *Ann. NY Acad. Sci.* 635:18–25.

Atchison, W.D., L. Adgate, and C.M. Beaman. 1988. Effects of antibiotics on uptake of calcium into isolated nerve terminals. *J. Pharmacol. Exp. Ther.* 245:394–401.

Bekoff, A., and W.J. Betz. 1977. Physiological properties of dissociated muscle fibers obtained from innervated and denervated adult rat muscle. *J. Physiol.* 271:25–40.

Bérdy, J., A. Aszalos, M. Bostian, and K. McNitt. 1980. *In* CRC Handbook of Antibiotic Compounds. Vol. 1. Carbohydrate Antibiotics. CRC Press, Inc., Boca Raton, FL. 33–176.

Blatz, A.L., and K.L. Magleby. 1988. Correcting single channel data for missed events. *Biophys. J.* 49:967–980.

Brasseur, R., G. Laurent, J-M. Ruysschaert, and P. Tulkens. 1984. Interaction of aminoglycoside antibiotics with negatively charged lipid layers. Biochemical and conformational studies. *Biochem. Pharmacol.* 33:629–637.

Caputy, A.J., Y.I. Kim, and D.B. Sanders. 1981. The neuromuscular blocking effects of therapeutic concentrations of various antibiotics on normal rat skeletal muscle: a quantitative comparison. *J. Pharmacol. Exp. Ther.* 217:369–378.

Chung, L., G. Kaloyanides, R. McDaniel, A. McLaughlin, and S. McLaughlin. 1985. Interaction of gentamicin and spermine with bilayer membranes containing negatively charged phospholipids. *Biochemistry.* 24:442–452.

Colquhoun, D., and F.J. Sigworth. 1983. Fitting and statistical analysis of single channel records. *In Single-Channel Recording.* B. Sakmann and E. Neher, editors. Plenum Publishing Corp., New York. 191–263.

Dorman, D.E., J.W. Paschal, and K.E. Merkel. 1976. ^{15}N nuclear magnetic resonance spectroscopy. The nebramycin aminoglycosides. *J. Am. Chem. Soc.* 98:6885–6888.

Dulon, D., G. Zajic, J.-M. Aran, and J. Schacht. 1989. Aminoglycoside antibiotics impair calcium entry but not viability and motility in isolated cochlear outer hair cells. *J. Neurosci. Res.* 24:338–346.

Dretchen, K.L., S.D. Gergis, M.P. Sokoll, and J.P. Long. 1972. Effect of various antibiotics on neuromuscular transmission. *Eur. J. Pharmacol.* 18:201–203.

Enomoto, K., and T. Maeno. 1981. Presynaptic effects of 4-aminopyridine and streptomycin on the neuromuscular junction. *Eur. J. Pharmacol.* 76:1–8.

Fieckers, J.F. 1983. Effects of the aminoglycoside antibiotics, streptomycin and neomycin, on neuromuscular transmission. I. Presynaptic considerations. *J. Pharmacol. Exp. Ther.* 225:487–495.

Gâbev, E., J. Kasianowicz, T. Abbott, and S. McLaughlin. 1989. Binding of neomycin to phosphatidylinositol 4,5-bisphosphate (PIP_2). *Biochim. Biophys. Acta* 979:105–112.

Hamill, O.P., A. Marty, E. Neher, B. Sakmann, and F.J. Sigworth. 1981. Improved patch-clamp techniques for high resolution current recordings from cells and cell-free membrane patches. *Pflügers Arch. Eur. J. Physiol.* 391:85–100.

Hess, P., and R.W. Tsien. 1984. Mechanism of ion permeation through calcium channels. *Nature (Lond.)* 309:453–456.

Hess, P., J.B. Lansman, and R.W. Tsien. 1986. Calcium channel selectivity for divalent and monovalent cations. Voltage and concentration dependence of single-channel current in ventricular heart cells. *J. Gen. Physiol.* 88:293–319.

Hino, H., R. Ochi, and T. Yanagisawa. 1982. Inhibition of the slow inward current and the time-dependent outward current of mammalian ventricular muscle by gentamicin. *Pflügers Arch. Eur. J. Physiol.* 394:243–249.

Josepovitz, C., E. Pastoriza-Munoz, D. Timmerman, M. Scott, S. Feldman, and G.J. Kaloyanides. 1982. Inhibition of gentamicin uptake in rat renal cortex in vivo by aminoglycosides and organic polycations. *J. Phar. Exp. Therap.* 223:314–321.

Kim, M.-S., T. Morii, L.X. Sun, S. Imoto, and Y. Mori. 1993. Structural determinants of ion selectivity in brain calcium channel. *FEBS Lett.* 318:145–148.

Kou, C.-C., and P. Hess. 1993*a*. Ion permeation through the L-type Ca^{2+} channel in rat phaeochromocytoma cells: two sets of ion binding sites in the pore. *J. Physiol.* 466:629–655.

Kou, C.-C., and P. Hess. 1993*b*. Characterization of the high-affinity Ca^{2+} binding sites in the L-type Ca^{2+} channel pore in rat pheochromocytoma cell. *J. Physiol.* 466:657–682.

Kroese, A.B.A., A. Das, and A.J. Hudspeth. 1989. Blockage of the transduction channels of hair cells in the bullfrog's sacculus by aminoglycoside antibiotics. *Hear. Res.* 37:203–218.

Lansman, J.B. 1990. Blockade of current through single calcium channels by trivalent lanthanide cations. Effect of ionic radius on the rates of ion entry and exit. *J. Gen. Physiol.* 95:679–696.

Lansman, J.B., P. Hess, and R.W. Tsien. 1986. Blockade of current through single Ca^{2+} channels by Cd^{2+}, Mg^{2+}, and Ca^{2+} voltage and concentration dependence of calcium entry into the pore. *J. Gen. Physiol.* 88:321–347.

Lüllmann, H., H. Plösch, and A. Ziegler. 1980. Ca replacement by cationic amphiphilic drugs from lipid monolayers. *Biochem. Pharmacol.* 29:2969–2974.

McCleskey, E.W., and W. Almers. 1985. The Ca channel in skeletal muscle is a large pore. *Proc. Natl. Acad. Sci. USA.* 82:7149–7153.

Neher, E., and J.H. Steinbach. 1978. Local anesthetics transiently block currents through single acetylcholine receptor channels. *J. Physiol.* 277:153–176.

Nomura, K., K. Naruse, K. Watanabe, and M. Sokabe. 1990. Aminoglycoside blockade of Ca^{2+}-activated K^+ channels from rat brain synaptosomal membranes incorporated into planar bilayers. *J. Membr. Biol.* 115:241–251.

Ohmori, H. 1985. Mechano-electrical transduction currents in isolated vestibular hair cells of the chick. *J. Physiol. (Lond.).* 359:189–217.

Pietrobon, D., B. Prod'hom, and P. Hess. 1989. Interactions of protons with single open L-type calcium channels: pH dependence of proton-induced current fluctuations with Cs^+, K^+, and Na^+ as permeant ions. *J. Gen. Physiol.* 94:1–21.

Sakon, J., H.H. Liao, A.M. Kanikula, M.M. Benning, I. Rayment, and H.M. Holden. 1993. Molecular structure of kanamycin nucleotidyltransferase determined to 3.0-Å resolution. *Biochemistry.* 32:11977–11984.

Singh, Y.N., I.G. Marshall, and A.L. Harvey. 1979. Depression of transmitter release and postjunctional sensitivity during neuromuscular block produced by antibiotics. *Br. J. Anaesth.* 51:1027–1033.

Suarez-Kurtz, G., and J.P. Reuben. 1987. Effects of neomycin on calcium channel currents in clonal GH3 pituitary cells. *Pflügers Arch. Eur. J. Physiol.* 410:517–523.

Timmerman, J., C.J.P. Long, and C.B. Pittenger. 1959. Neuromuscular blocking properties of various antibiotic agents. *Toxicol. Appl. Pharmacol.* 1:299–304.

Tsien, R.W., P. Hess, E.W. McCleskey, and R.L. Rosenberg. 1987. Calcium channels: mechanisms of selectivity, permeation, and block. *Annu. Rev. Biophys. Biophys. Chem.* 16:265-290.

Wagner, J., A.M. Snowman, B.M. Olivera, and S. Snyder. 1987. Aminoglycoside effects on voltage-sensitive calcium channels and neurotoxicity. *N. Eng. J. Med.* 317:1669.

Winegar, B.D., R. Kelly, and J.B. Lansman. 1991. Block of current through single calcium channels by Fe, Co, and Ni. Location of the transition metal binding site within the pore. *J. Gen. Physiol.* 97:351–367.

Winegar, B.D., C.M. Haws, and J.B. Lansman. 1992. Aminoglycoside antibiotic block of single mechanosensitive and L-type Ca^{2+} channels. *Biophys. J.* 61:A304. (Abs.)

Woodhull, A. 1973. Ionic blockage of sodium channels in nerve. *J. Gen. Physiol.* 61:687–708.

Wright, J.M., and B. Collier. 1977. The effects of neomycin on transmitter release and action. *J. Pharmacol. Exp. Ther.* 200:576–587.

Yang, J., P.T. Ellinor, W.A. Sather, J.-F. Zhang, and R.W. Tsien. 1993. Molecular determinants of Ca^{2+} selectivity and ion permeation in L-type Ca^{2+} channels. *Nature (Lond.).* 366:158–161.